NMR IN BIOMEDICINE, VOL. 7, 69–74 (1994)

Potential Pitfalls of Functional MRI using Conventional Gradient-Recalled Echo Techniques

Seong-Gi Kim,†* Kristy Hendrich,‡ Xiaoping Hu,† Hellmut Merkle† and Kâmil Uğurbil†‡§

Center for Magnetic Resonance Research, Departments of †Radiology, ‡Biochemistry and §Medicine, University of Minnesota Medical School, 385 E. River Road, Minneapolis, MN 55455, USA

The conventional gradient-recalled echo technique, FLASH, has widely been used for functional MRI. FLASH results at 4 T with short *TE*s of 10–20 ms mimic those at 1.5 T with *TE*s of 25–50 ms or longer. Under these conditions, large venous vessels dominate the activated area; however, the use of longer *TE*s at 4 T reveals activation in gray matter areas as well as large vessels. Inflow effects of large vessels can be greatly reduced with centric-reordering of phase-encoding steps and inter-image delay. Finger and toe movement paradigms show that functional activation maps are consistent with classical somatotopic maps, and are specific to the tasks. Navigator-based motion correction generates functional maps with larger activation areas by reducing physiological noise.

INTRODUCTION

Since its inception in 1973,[1] MRI has evolved into one of the most powerful techniques in diagnostic clinical medicine and biomedical research. A very significant recent development has been the use of MRI to non-invasively map human cortical function with the use of endogenous blood oxygenation level dependent (BOLD) contrast.[2–17] The basis of this technique is that deoxyhemoglobin acts as an endogenous paramagnetic contrast agent.[18,19] Therefore, changes in the local concentration of deoxyhemoglobin within the brain lead to alterations in the MR image signal.[20–22] Neuronal activation within the cerebral cortex leads to an increase in blood flow without an increase of similar magnitude in oxygen extraction.[23] Consequently, the deoxyhemoglobin concentrations decrease, resulting in an increase in T_2^* and T_2, as well as in signal intensity of T_2^*- and T_2-weighted MR images.

The BOLD effect can in principle arise from capillaries, venules, and veins, all of which contain deoxyhemoglobin. The effect, however, depends on the blood vessel diameter. For small vessels such as capillaries and venules, BOLD is dominated by alterations in transverse relaxation (T_2), since diffusion-averaging becomes the major contributor to signal loss.[24] By contrast, tissue adjacent to large venous vessels experiences predominantly susceptibility-induced dephasing (T_2^*) rather than changes of T_2 relaxation.[24]

Despite early documentation of the BOLD effect in response to changing deoxyhemoglobin content[18,20,22] in animals, and calculations predicting the BOLD effect in humans,[2,24] the origin of the functional brain 'activation' maps generated by gradient echo-based images has been unclear and controversial. Imaging sequences employed in functional mapping can exhibit signal intensity changes simply due to perturbations in blood flow (the 'inflow' effect). This provides an alternative mechanism for the task-related signal intensity changes seen in functional imaging studies with MR. The inflow contribution was corroborated by many early experiments at low fields that detected large task-induced fractional changes in signal intensity; although signal changes are expected to depend on spatial resolution, paradigms, etc., large signal changes at low magnetic field strength cannot be easily explained by the BOLD mechanism.[24,25] We documented[17] that the BOLD effect as opposed to inflow or task-related artifact is the origin of photic stimulation-induced signal intensity changes in our 4 T studies by directly measuring T_2^* changes; this study, however, also demonstrated that during increased neuronal activity the most prominent BOLD changes were associated with large venous vessels even at 4 T. This observation together with the expected field dependence on diameter of blood vessel led to the conclusion that functional activation at low magnetic fields, especially at short *TE*s, is likely to be dominated by large vessel contributions and/or inflow effects from large venous and arterial vessels; in the 4 T photic stimulation studies,[17] however, gray matter area devoid of detectable vessels in high-resolution images was also activated, documenting the presence of a task-specific BOLD effect associated with small blood vessels such as capillaries and venules. Lai *et al.*[26] provided experimental evidence that large drainage vessels are the only source of functional activation of the human motor cortex at the clinical field strength of 1.5 T, and extrapolated the claim to higher magnetic fields (4 T).

In addition to the vascular origin (and in fact related to it), an important issue to consider in MR functional imaging is the origin and the nature of the 'noise' in the consecutive images from which an 'activation' map is generated. Physiological noise (such as that caused by vascular and brain pulsation) is the dominant contribution to inter- and intra-image signal intensity fluctuation when instrumental contributions are minimized. Furthermore, the inter-image fluctuation is higher in

* Author to whom correspondence should be addressed.

Abbreviations used: BOLD, blood oxygenation level dependent; PCM, per cent signal intensity change map.

CCC 0952–3480/94/010069–06

Received 2 November 1993
Accepted (revised) 8 November 1993

gray matter than in white matter,[27,28] and these oscillations arise primarily at the frequencies of the heart beat and the respiration.[27] Image intensity fluctuation may appear as artifactual activation in the functional image or degrade the ability to detect low level activation related to signal changes with adequate statistical confidence. It is expected that these signal intensity oscillations in a given voxel will also depend on the type and size of blood vessels present within a voxel.

The aforementioned issues raise concerns about the spatial accuracy and specificity of MR-based functional imaging. We have examined these issues in the human motor cortex at 4 T. The motor cortex is in close proximity to large arterial and venous vessels that traverse the surface of the brain near the central sulcus; therefore, functional imaging studies of the motor cortex are particularly susceptible to inflow and BOLD effects of large venous vessels. It is also well recognized that the motor cortex is organized so as to control different parts of the body in spatially distinct regions of the cortex. Thus, the motor cortex provides an ideal test for specificity.

Using standard gradient echo techniques, we assess (i) whether or not functional activation sites reside solely in large vessels at 4 T, (ii) how the BOLD effect can be separated from the inflow effect, (iii) whether functional activation is specific to the task, and (iv) how physiological noise can be reduced.

METHODS

Data collection

MRI studies were performed with a 4 T whole body imaging system with actively shielded gradient coils and a 1.25 m diameter horizontal bore (SIS Co., Sunnyvale, CA; Siemens, Erlangen, Germany). RF power deposition was kept below FDA specific absorption rate guidelines. An anatomically fitted surface coil was used for MRI signal detection.[29] Human volunteers were recruited from the academic environment of the University of Minnesota Medical School.

To locate the primary motor cortex (precentral gyrus), multislice T_1-weighted axial images were obtained using a magnetization prepared ultrafast gradient-recalled echo imaging technique[30] with a TE of 10 ms, TR of 20 ms and inversion time of 1.2 s. From these images, an oblique slice between axial and sagittal planes was defined along the central sulcus on the left hemisphere; in the oblique plane, the precentral gyrus was located anterior to the central sulcus.[3,4] The oblique plane was verified by multislice oblique anatomic images, obtained using the Turbo-FLASH imaging technique with 256 centric-recorded phase-encoding steps, segmented in four blocks of 64 interleaved steps. In each slice acquired for functional studies, both anatomic and flow-weighted high-resolution images were collected, typically with a 256×256 matrix size. Flow-weighted images were acquired using a T_2^*-weighted FLASH sequence with 256 linear phase-encoding steps and a flip angle of 45°.

Consecutive T_2^*-weighted images were collected using a refocused FLASH sequence,[31] first under a resting 'non-stimulated' state, then during a 'task' period, and ending with a 'non-stimulated' recovery state. Usually 10 images were acquired in each period. Typical imaging parameters were $TE = 38$ ms, $TR = 55$ ms, inter-scan delay = 2 s, flip angle = 11° and slice thickness = 6–12 mm. Generally 128 complex pairs in the readout direction and 64 phase-encoding steps were acquired in a 16×13 cm^2 field of view. Tasks were repetitive, sequential right finger movements between thumb and the remaining four digits or right toe movements. The time to start and to stop the movements was indicated by a light-emitting diode placed inside the magnet bore in front of the subject.

Three different experimental conditions were tested to determine sources of functional activation. In the first case, eight gradient echoes were collected to examine the relationship between functional activation and gradient-echo time in the motor cortex. The shortest TE was 11 ms, the interval between consecutive echoes was 6.8 ms, and the longest TE was 59 ms. Four-scan averaging was used with 6 mm slice thickness and centric-recorded phase-encoding steps. In the second case, centric ($k = 0, \pm 1, \pm 2$, etc.) and linear phase-encoding orders were tested under identical conditions to determine the contribution of inflow effect to the functional activation map. Single scans were acquired with a slice thickness of 12 mm. In the third case, finger and toe movements were performed as separate tasks by the same subject to verify that functional activation sites are consistent with classical somatotopic electrical stimulation maps. Imaging parameters were the same as for the second case, except that only centric-reordered phase-encoding steps were used.

In order to reduce physiological image fluctuations, a single complex data point was collected before phase-encoding and readout gradients were applied, and its phase was used to correct subsequently acquired k-space lines.[37] Functional activation maps were generated both with and without this navigator echo-based motion correction for comparison.

Data processing

The T_2^*-weighted data were zero-filled to 256×256, then Fourier-transformed. A per cent signal intensity change map (PCM) was calculated by comparing T_2^*-weighted images acquired during baseline resting conditions and during tasking. The difference between average baseline and average task-induced image intensities was calculated and normalized by the corresponding baseline image intensity on a pixel-by-pixel basis. The baseline image intensity was obtained by averaging the pre- and post-task images. Since hemodynamic response time to the task was ca 7–10 s,[3,6,7] images collected within 10 s following the beginning and end of task were not included for task and post-task images, respectively. For example, if the total time for each image was ca 5 s, the first two images acquired after initiation and cessation of task were not included for task and post-task images, respectively. The following two criteria determined activation: (i) the Student's t-test was performed to compare the baseline and movement-related intensity at a desired confidence level; only pixels with a statistically significant activation were included in the PCM,[3,4,14] and (ii) regions with less than eight contiguous activated pixels were not

included in the PCM, since a single pixel of the raw data (128 × 64) approximately corresponded to 8 pixels in the zero-filled image (256 × 256). Then, the PCM was overlaid on a T_1-weighted anatomic image to locate the activation site, and also overlaid on a flow-weighted image to determine whether or not the activation's origin was from large vessels.

RESULTS AND DISCUSSION

Echo time dependency and vessel contributions

Plate 1 shows the dependence on gradient-echo time of the functional activation maps for finger movements, which are overlaid on the flow-weighted images. Dark areas in the flow-weighted images are venous vessels, which have large BOLD effects. At short *TE* of 11 ms, the activation is predominantly located at vessels large enough to be directly visualized in high-resolution T_2^*-weighted images; these 'large' vessels are greater than the in-plane resolution of 0.6 mm × 0.5 mm, and include the superior sagittal sinus. At longer *TE*, activation is present both in regions devoid of such large vessels, as well as in large vessels. Per cent signal changes of the activated areas increased linearly with *TE*, as expected.[17,24]

A large vessel may exert a susceptibility influence on an adjacent slice, while not being easily detectable within the flow-weighted image of the adjacent slice. Thus, to determine the source of activation, one should compare the activation map with flow-weighted images of both the corresponding and neighboring slices. In our study, adjacent slices were examined to take account of such effects; activation at long *TE* was seen in some regions where there were no large vessels in either the corresponding slice or the adjacent slices.

Lai *et al.*[26] showed that activation of the motor cortex came from large vessels at 1.5 T, and claimed that all functional activation originated solely from large vessels, even at high magnetic fields. However, our results demonstrate that with long *TEs* at 4 T, small but detectable signal changes due to functional activation are seen in areas lacking large venous vessels and are associated with gray matter; this effect must arise from vessels smaller than the image resolution in these studies (0.6 mm × 0.5 mm in plane resolution and 6 mm slice thickness). These observations are consistent with recent experimental studies of visual cortex by Menon *et al.*[17] and simulation by Ogawa *et al.*[24]

Our calculations[24] demonstrated that the BOLD phenomenon has two components, one dependent linearly on the static magnetic field (B_0) and the other varying quadratically with B_0; the former is due to dephasing of the magnetization in the presence of susceptibility-induced gradients of venous vessels >10 μm in diameter, and the latter is due to diffusion within the steep, susceptibility-induced gradients from small vessels (capillaries and venules). These calculations imply that short *TEs* of 10–20 ms at 4 T mimic longer *TEs* of 25–50 ms at 1.5 T for the large vessel contribution, and 70–140 ms for the small vessel contribution.[24] Almost all present lower field functional imaging studies have been performed with *TEs* of 25–50 ms. Therefore, our *TE* dependence in the motor cortex suggests that at low fields and short *TEs*, the T_2^*-weighted BOLD phenomenon arises predominantly from large vessels (e.g., ca 1 mm diameter); this effectively introduces a physiological limitation on the spatial resolution of the functional images, since such vessels are not uniformly and densely distributed in the brain.

In order to locate activation sites, a functional map is commonly overlaid on an anatomic image. If the activation site corresponds to a gray matter area or a sulcus in the anatomic image, then the activation is assumed to be at parenchyma or vessel, respectively. However, many large vessels run over gyri, especially on the surface of brain, e.g., the Rolandic vein traverses the precentral gyrus, and both gyrus and the adjacent vessels can exist within an imaging slice. Thus, identification of activation sites should not rely on an anatomic image, but also on a flow-weighted image. An example of this situation is shown in Plate 2, where functional activation is overlaid on both anatomic and flow-weighted images. The functional activation indicated by red arrows appears to originate from gray matter (anatomic image), but actually originates from a large venous vessel (flow-weighted image). One should be cautious in concluding that there is activation of gray matter if flow-weighted images are not available for comparison.

It is also possible to evaluate the vascular origin of activation sites in the absence of flow-weighted images. Our measurements demonstrate that signal fluctuation in large vessel areas is generally greater than that of gray and white matter, possibly due to the pulsatile motion of the vessels. Furthermore, large venous vessels have large BOLD effects (i.e., less signal) and marked signal changes at the boundary. Consequently, large vessels are more sensitive than gray and white matter areas to any brain motion. The signal fluctuation within a pixel in consecutive images can be quantified as the per cent SD (100 × SD/mean) for that pixel. Plate 3 shows a comparison between a flow-weighted image and a per cent SD map corresponding to the resting (baseline) condition on the same subject. Areas of high fluctuation in the per cent SD map correspond very well with large vessels in the flow-weighted image. These SD maps may be helpful in determining the location of large vessels.

Inflow effect

When either FLASH or echo planar imaging sequences are repeated rapidly compared to T_1, it is possible to induce signal intensity changes due to the inflow effect, secondary to increased blood flow; this inflow effect will also have large vessel contributions and is most likely a major contributor to the large changes reported at low magnetic fields. Linear phase-encoding steps with a high flip angle, commonly used for functional imaging,[11,12] are very sensitive to inflow effects.[32] With linear phase-encoding, low *k*-space lines are sampled during a condition of steady state magnetization, therefore, the fresh, non-saturated inflowing spins increase signal intensity within the FLASH image. Generally, higher flip angles are more sensitive to inflow effects in single-slice or multislice imaging (but not in 3D). Gao *et al.*[32] reported a detailed theoretical description of signal intensity of moving spins in a FLASH image,

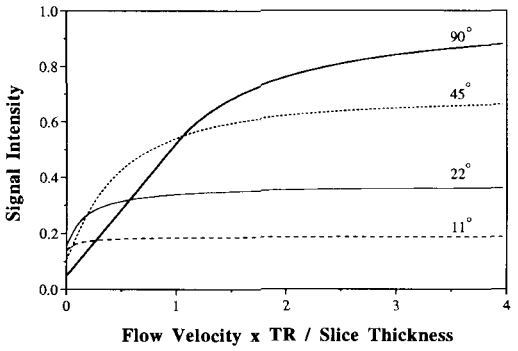

Figure 1. Theoretical relationship between signal intensity [in units of $//M_0\pi a^2 L$; see Eqn (35) of Ref 32] and flow of the center of the vessel (in units of flow velocity × *TR*/slice thickness), for TR/T_1 of 0.05, and four different flip angles of 11, 22, 45 and 90°.

which is dependent on various parameters, including slice thickness, *TR* and flow velocity. Figure 1 shows the theoretical relationship between signal intensity and inflow, based on the results of Gao *et al.*,[32] for TR/T_1 of 0.05. When $TR = 50$ ms, $T_1 = 1$ s, slice thickness = 5 mm, and flow velocity increases from 2.0 to 3.0 cm/s, as is typical for small venous vessels and arterioles (between 0.2 and 0.3 on the horizontal axis of Fig. 1), the signal intensity increase is ca 2, 8, 23 and 33% for flip angles of 11, 22, 45 and 90°, respectively. Thus, stimulation-induced flow increase can cause a considerable signal increase in the image intensity of the macrovasculature. This inflow effect should be distinguished from the BOLD effect, and ideally eliminated.

Centric-reordered phase-encoding steps ($k = 0, +1, -1, +2, -2$, etc.) with a low flip angle and an inter-image delay, as used in this laboratory,[2,5,14,17] minimize the inflow effects. Since the low *k*-space lines, which contribute most to the signal intensity and contrast,[33] are collected first, before a steady state is reached, image intensity is determined by the inter-image delay and the flip angle. During the inter-image delay, all the spins in vessels with flow velocity greater than slice thickness/delay are replenished by fresh spins. When an inter-image delay is relatively long, image intensity is essentially independent of flow. This is the case with the 2 s inter-image delay in this study. Thus, flow velocity change (inflow effect) does not induce significant signal intensity alteration. Note though, that centric-recorded phase-encoding is more sensitive than linear phase-encoding to gross motion (see below).

Plate 4 shows FLASH functional activation maps with centric-reordered and linear phase-encoding steps overlaid on flow-weighted images. High resolution images (0.6 mm × 0.5 mm in plane resolution, 6 mm slice thickness) with a linear phase-encoding order and a high flip angle (45°) show bright signal at the inflow area due to movement of spins into the imaging slice. Thus, inflow vessels can be easily identified in high-resolution T_2^*-weighted images. Clearly, the functional images with linear phase-encoding steps show activation at these bright inflow areas, as well as the additional areas of activation seen in the images with centric-recorded phase-encoding steps.

An alternative approach to eliminate inflow effects in gradient-recalled echo images is the T_2^*-weighted Turbo-FLASH sequence described by us.[34] A crushing gradient and a delay period between magnetization preparation and data collection will dephase the spins undergoing flow and diffusion; thus fast-moving components will selectively lose signal, in contrast to slow-moving components and stationary tissue.

Specificity

We have shown that the functional activation seen at 4 T with the conventional gradient-echo technique originates from both large vessels and gray matter. One important question therefore, is whether the activation is task-specific. Nine volunteers were successfully studied during both finger and toe movements. Plate 5 shows functional activation maps generated from the toe and finger movement paradigms from one volunteer. In these studies, only centric-reordered phase-encoding steps were used to minimize the inflow effect. Clearly the finger motor area, which is the lateral and posterior wall of the precentral gyrus, shows activation only during the finger movements, and not during the toe movements. One subject showed activation along most of the draining vessels within the central sulcus during finger movements. In some subjects, the medial area was also activated, to a lesser extent, during finger movements. Medial activation may arise from the medial supplementary motor area and the medial premotor area.[35] During toe movements, the medial motor area (close to the midline) activated in all nine volunteers. These results are consistent with classical somatotopic maps.[36] Even though the task-induced signal changes originate primarily from the BOLD effect due to large venous vessels, the functional activation is task-specific.

Motion correction

Both inter- and intra-image fluctuations are problematic in functional imaging, where physiological noise such as brain pulsation can be a dominant source of fluctuation. The task-induced signal change is of the same order as baseline noise, and we must detect task-induced signal intensity increases that are statistically significant relative to the intensity fluctuations. It has been qualitatively observed that the inter-image fluctuation may be lower in functional MRI implemented with echo planar imaging and Turbo-FLASH as compared to conventional FLASH.[2,3,6,7,34] Echo planar imaging effectively obtains a snapshot of the brain frozen in time, and similarly Turbo-FLASH is collected relatively quickly. However, a FLASH image is acquired during several cardiac and respiratory cycles. Each *k*-space line in a single image is therefore collected at a different place in one of these cycles, causing the phase of the MRI echo to vary. Consequently, this leads to phase inconsistencies between successive lines of *k*-space and image-to-image variations.

We have developed a navigator echo-based motion correction scheme which minimizes the phase inconsistency among *k*-space lines.[37] Acquisition of a single complex data pair immediately precedes phase and readout gradient-encoding, and the phase of this pair is used to correct the phase of subsequently acquired *k*-space lines, directly minimizing *k*-space fluctuations

and subsequently reducing inter-image fluctuations. We evaluated the signal variations during a series of FLASH images using this navigator echo-based technique. Plate 6 shows functional activation maps of the motor cortex generated in response to finger movements both with and without navigator echo-based motion correction. The navigator echo method significantly reduced the signal fluctuations between images; therefore small task-induced signal increases in gray matter were statistically significant, and the functional map shows a larger activation area in gray matter regions (verified with flow-weighted images—data not shown). Without correction, the predominant activation seen in these functional maps is due to large signal changes (as in vessels).

The signal change seen in high-resolution functional imaging is especially sensitive to *gross* inter-image motion, therefore it is necessary to identify the presence of motion-induced fluctuations, so that signal changes which are not task-specific can be rejected. Such artifacts may be minimized with image registration techniques, although their application was not employed here. Artifacts induced by head movements usually appear as global spatially interleaved positive and negative patterns in functional image intensity,[4] therefore they can be identified and rejected. Since centric-reordered phase-encoding is sensitive to motion, its usage is helpful both in detecting gross motion-induced fluctuations as well as minimizing inflow effects (see above).

CONCLUSIONS

In functional imaging, the task-induced signal intensity change is greater at high magnetic field strengths, especially for the capillary,[24,25] and physiological noise is independent of magnetic field strength.[27] Taken together, these observations suggest that a high magnetic field is advantageous for functional imaging, especially for microvascular-based functional imaging.

Functional MRI of the motor cortex at 4 T using FLASH shows activation from predominantly large venous vessels at short *TE*s of 10–20 ms, and from gray matter areas as well as large vessels at longer *TE*s. We have also shown that inflow effects can be minimized using low RF pulse flip angles, a centric-reordered phase-encoding step and inter-image delays. Although task-induced signal changes are due to the BOLD effect from both large drainage vessels and gray matter in the absence of inflow effects, functional activation is specific to the paradigm. Improved functional maps with larger activation areas can be generated with navigator-based motion correction.

Acknowledgements

We thank Drs R. Menon, J. Ashe and A. Georgopoulos for their helpful discussions. This work was supported by NIH Grants RR08079, HL32427 and HL33600 and by the Whitaker foundation (to XH).

REFERENCES

1. Lauterbur, P. C. Image formation by induced local interaction: examples employing nuclear magnetic resonance. *Nature* **242**, 190–191 (1973).
2. Ogawa, S., Tank, D. W., Menon, R., Ellermann, J. M., Kim, S.-G., Merkle, H. and Ugurbil, K. Intrinsic signal changes accompanying sensory stimulation: functional brain mapping with magnetic resonance imaging. *Proc. Natl Acad. Sci. USA* **89**, 5951–5955 (1992).
3. Kim, S.-G., Ashe, J., Georgopoulos, A. P., Merkle, H., Ellermann, J. M., Menon, R. S., Ogawa, S. and Ugurbil, K. Functional imaging of human motor cortex at high magnetic field. *J. Neurophysiol.* **69**, 297–302 (1993).
4. Kim, S.-G., Ashe, J., Hendrich, K., Ellermann, J. M., Merkle, H., Ugurbil, K. and Georgopoulos, A. P. Functional magnetic resonance imaging of motor cortex: hemispheric asymmetry and handedness. *Science* **261**, 615–617 (1993).
5. Menon, R. S., Ogawa, S., Kim, S.-G., Ellermann, J. M., Merkle, H., Tank, D. W. and Ugurbil, K. Functional brain mapping using magnetic resonance imaging signal changes accompanying visual stimulation. *Invest. Radiol.* **27**, S47–S53 (1992).
6. Bandettini, P. A., Wong, E. C., Hinks, R. S., Tikofsky, R. S. and Hyde, J. S. Time course EPI of human brain function during task activation. *Magn. Reson. Med.* **25**, 390–398 (1992).
7. Kwong, K. K., Belliveau, J. W., Chesler, D. A., Goldberg, I. E., Weisskoff, R. M., Poncelet, B. P., Kennedy, D. N., Hoppel, B. E., Cohen, M. S., Turner, R., Cheng, H.-M., Brady, T. J. and Rosen, B. R. Dynamic magnetic resonance imaging of human brain activity during primary sensory stimulation. *Proc. Natl Acad. Sci. USA* **89**, 5675–5679 (1992).
8. Blamire, A. M., Ogawa, S., Ugurbil, K., Rothman, D., McCarthy, G., Ellermann, J. M., Hyder, F., Rattner, Z. and Shulman, R. G. Dynamic mapping of the human visual cortex by high-speed magnetic resonance imaging. *Proc. Natl Acad. Sci. USA* **89**, 11069–11073 (1992).
9. Turner, R. Magnetic resonance imaging of brain function. *Am. J. Physiol. Imag.* in press.
10. Turner, R., Jezzard, P., Wen, H., Kwong, K. K., Le Bihan, D., Zeffiro, T. and Balaban, R. S. Functional mapping of the human visual cortex at 4 and 1.5 Tesla using deoxygenation contrast EPI. *Magn. Reson. Med.* **29**, 277–279 (1993).
11. Frahm, J., Bruhn, H., Merboldt, K.-D., Hanicke, W. and Math, D. Dynamic MR imaging of human brain oxygenation during rest and photic stimulation. *J. Magn. Reson. Imag.* **2**, 501–505 (1992).
12. Frahm, J., Merboldt, K.-D. and Hanicke, W. Functional MRI of human brain activation at high spatial resolution. *Magn. Reson. Med.* **29**, 139–144 (1993).
13. McCarthy, G., Blamire, A. M., Rothman, D. L., Gruetter, R. and Shulman, R. G. Echo-planar magnetic resonance imaging studies of frontal cortex activation during word generation in humans. *Proc. Natl Acad. Sci. USA* **90**, 4952–4956 (1993).
14. Hinke, R. M., Hu, X., Stillman, A. E., Kim, S.-G., Merkle, H., Salmi, R. and Ugurbil, K. Functional magnetic resonance imaging of Broca's Area during internal speech. *NeuroReport* **4**, 675–678 (1993).
15. Cao, Y., Towle, V. L., Levin, D. N. and Balter, J. M. Functional mapping of human motor cortical activation by conventional MRI at 1.5 T. *J. Magn. Reson. Imag.* in press.
16. Schneider, W., Noll, D. C. and Cohen, J. D. Functional topographic mapping of the cortical ribbon in human vision with conventional MRI scanners. *Nature* **365**, 150–153 (1993).
17. Menon, R. S., Ogawa, S., Tank, D. W. and Ugurbil, K. 4 Tesla gradient recalled echo characteristics of photic stimulation-induced signal changes in the human primary visual cortex. *Magn. Reson. Med.* **30**, 380–386 (1993).
18. Ogawa, S. and Lee, T.-M. Magnetic resonance imaging of blood vessels at high fields: *in vivo* and *in vitro* measurements and image simulation. *Magn. Reson. Med.* **16**, 9–18 (1990).
19. Thulborn, K. R., Waterton, J. C., Mattews, P. M. and Radda, G. K. Oxygenation dependence of the transverse relaxation time of water protons in whole blood at high field. *Biochem. Biophys. Acta* **714**, 265–270 (1982).

20. Ogawa, S., Lee, T.-M., Nayak, A. S. and Glynn, P. Oxygenation-sensitive contrast in magnetic resonance image of rodent brain at high magnetic fields. *Magn. Reson. Med.* **14**, 68–78 (1990).
21. Ogawa, S., Lee, T.-M., Kay, A. R. and Tank, D. W. Brain magnetic resonance imaging with contrast dependent on blood oxygenation. *Proc. Natl Acad. Sci. USA* **87**, 9868–9872 (1990).
22. Turner, R., Le Bihan, D., Moonen, C. T., Despres, D. and Frank, J. Echo-planar time course MRI of cat brain oxygenation changes. *Magn. Reson. Med.* **22**, 159–166 (1991).
23. Fox, P. T. and Raichle, M. E. Focal physiological uncoupling of cerebral blood flow and oxidative metabolism during somatosensory stimulation in human subjects. *Proc. Natl Acad. Sci. USA* **83**, 1140–1144 (1986).
24. Ogawa, S., Menon, R. S., Tank, D. W., Kim, S.-G., Merkle, H., Ellermann, J. M. and Ugurbil, K. Functional brain mapping by blood oxygenation level-dependent contrast magnetic resonance imaging: a comparison of signal characteristics with a biophysical model. *Biophys. J.* **64**, 803–812 (1993).
25. Weisskoff, R. M., Boxerman, J. L., Zuo, C. S. and Rosen, B. R. Endogenous susceptibility contrast: principles of relationship between blood oxygenation and MR signal change. In *Syllabus of Functional MRI of the Brain*, pp. 103–110 (1993).
26. Lai, S., Hopkins, A. L., Haacke, E. M., Li, D., Wasserman, B. A., Buckley, P., Friedman, L., Meltzer, H., Hedera, P. and Friedland, R. Identification of vascular structures as a major source of signal contrast in high resolution 2D and 3D functional activation imaging of the motor cortex at 1.5 T: preliminary results. *Magn. Reson. Med.* **30**, 387–392 (1993).
27. Jezzard, P., LeBihan, D., Cuenod, C., Pannier, L., Prinster, A. and Turner, R. An investigation of the contribution of physiological noise in human functional MRI studies at 1.5 Tesla and 4 Tesla. *12th Annual Meeting of the Society of Magnetic Resonance in Medicine.* Abstr., p. 1392 (1993).
28. Weisskoff, R. M., Baker, J., Belliveau, J., Davis, T. L., Kwong, K. K., Cohen, M. S. and Rosen, B. R. Power spectrum analysis of functionally-weighted MR data: what's in the noise? *12th Annual Meeting of the Society of Magnetic Resonance in Medicine.* Abstr., p. 7 (1993).
29. Merkle, H., Garwood, M. and Ugurbil, K. Dedicated circularly polarized surface coil assemblies for brain studies at 4 T. *12th Annual Meeting of the Society of Magnetic Resonance in Medicine.* Abstr., p. 1358 (1993).
30. Haase, A. Snapshot FLASH MRI: application to T_1, T_2, and chemical shift imaging. *Magn. Reson. Med.* **13**, 77–89 (1990).
31. Haase, A., Frahm, J., Matthaei, D., Hanicke, W. and Merboldt, K.-D. FLASH imaging. Rapid NMR imaging using low flip angle pulses. *J. Magn. Reson.* **67**, 258–266 (1986).
32. Gao, J.-H., Holland, S. K. and Gore, J. C. Nuclear magnetic resonance signal from flowing nuclei in rapid imaging using gradient echoes. *Med. Phys.* **15**, 809–814 (1988).
33. Chien, D., Atkinson, D. J. and Edelman, R. R. Strategies to improve contrast in TurboFLASH imaging: reordered phase encoding and K-space segmentation. *J. Magn. Reson. Imag.* **1**, 63–70 (1991).
34. Hu, X. and Kim, S.-G. A new T_2* weighting technique for magnetic resonance imaging. *Magn. Reson. Med.* **30**, 512–517 (1993).
35. Dum, R. P. and Strick, P. L. The origin of corticospinal projections from the premotor areas in the frontal lobe. *J. Neurosci.* **11**, 667–689 (1991).
36. Penfield, W. and Boldrey, E. Somatic motor and sensory representation in the cerebral cortex of man as studied by electrical stimulation. *Brain* **60**, 389–443 (1937).
37. Hu, X. and Kim, S.-G. Reduction of signal eluctuation in functional MRI using navigator echo. *Magn. Reson. Med.* in press (1994).

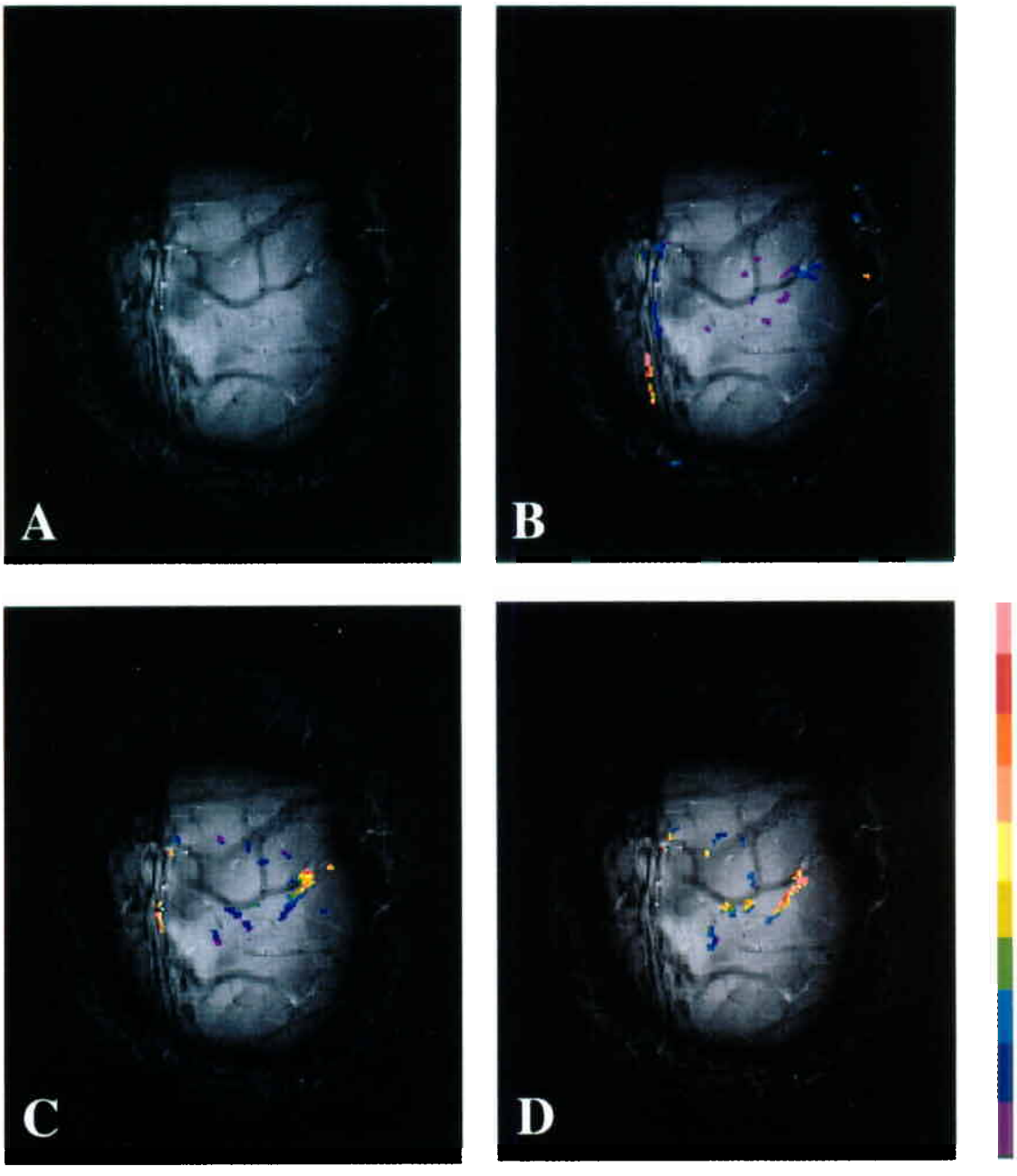

Plate 1. Dependence of gradient-echo time of functional activation maps ($p<0.01$) for finger movements. A high-resolution flow-weighted image is shown in (A). Functional activation maps were overlaid on flow-weighted images where TE=11 ms (B), TE=32 ms (C), and TE= 59 ms (D). Each color represents a 2% activation increment, starting at 2%. Note that at TE=11 ms, activation appears at large vessels including the superior sagittal sinus, but at 32 ms the activation appears at both large vessels and gray matter. Top is anterior.

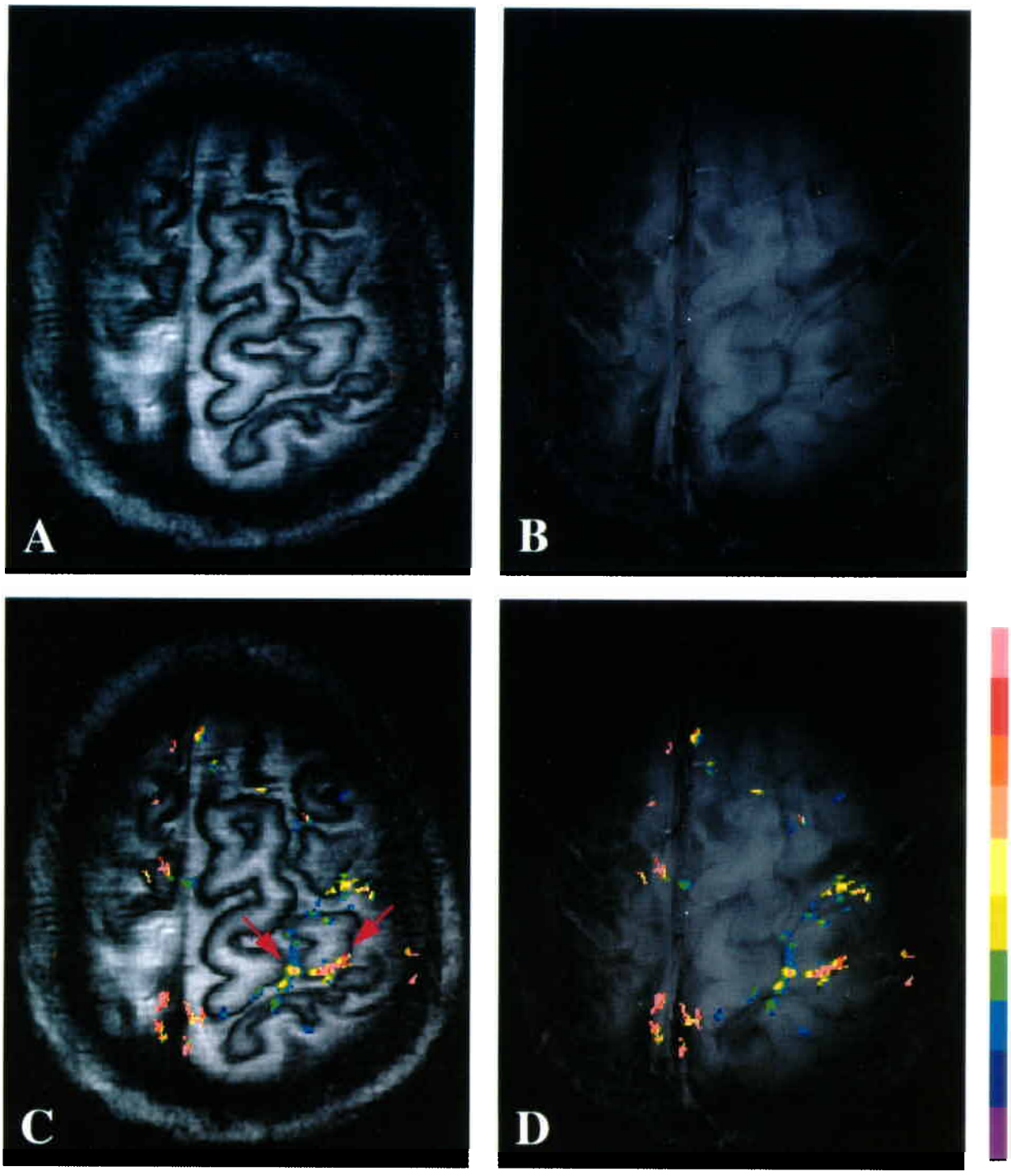

Plate 2. Anatomic T_1-weighted image (A), flow weighted image (B), and functional activation maps ($p<0.01$) during finger movements, overlaid on both anatomic (C) and flow-weighted images (D). Red arrows indicate the activated area, which appeared to be located in gray matter (C) but actually corresponded to a large venous vessel (D). Each color represents a 1% activation increment, starting at 1%. Top is anterior.

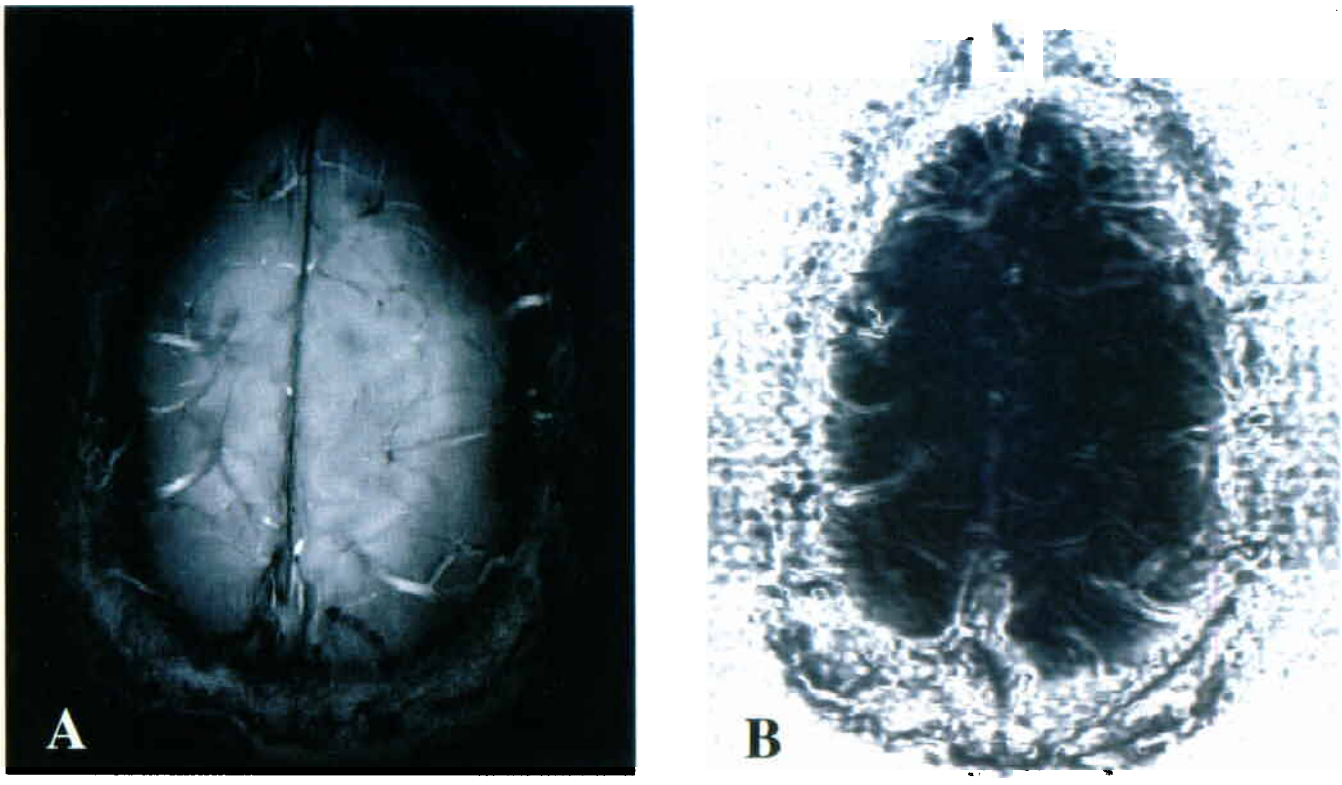

Plate 3. Flow weighted image (A) and per cent SD map (B) generated from baseline images. Areas with large SD correspond very well with the large vessels. Top is anterior.

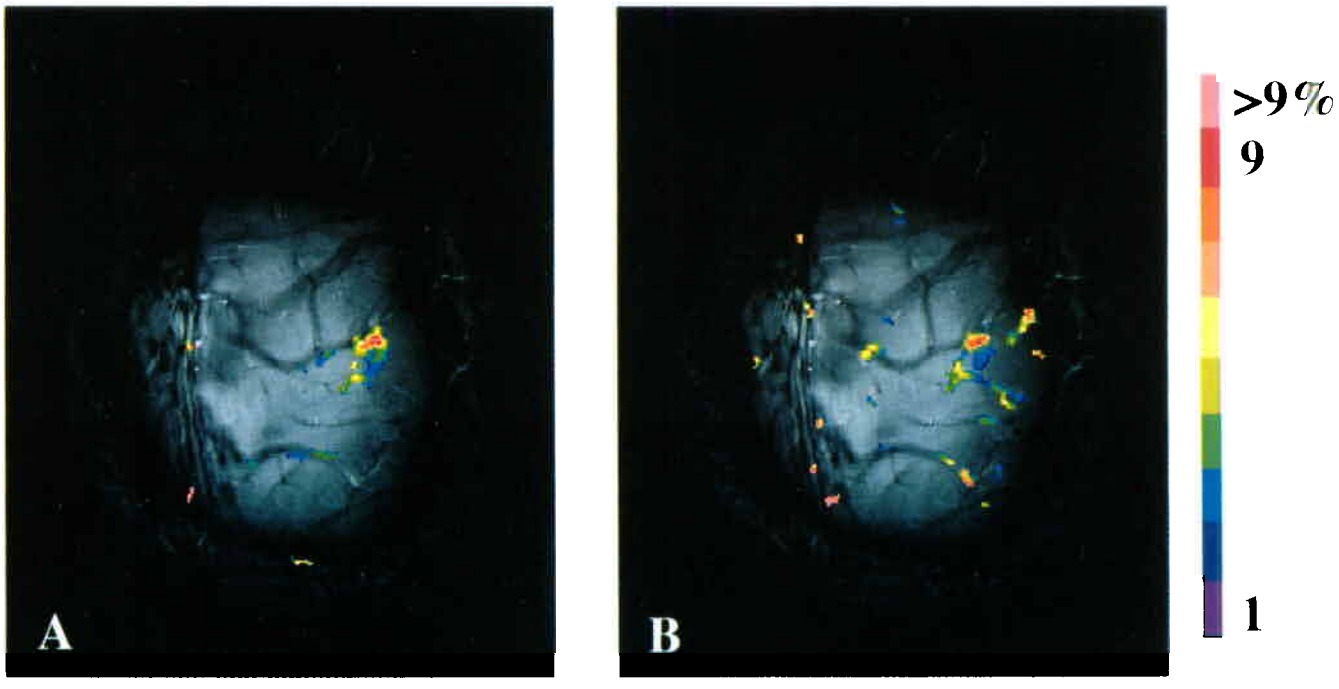

Plate 4. Functional activation maps of finger movements ($p<0.01$), overlaid on the flow weighted images, with centric reordered phase-encoding steps (A) and linear phase-encoding steps (B). Phase-encoding is along the horizontal direction and top is anterior.

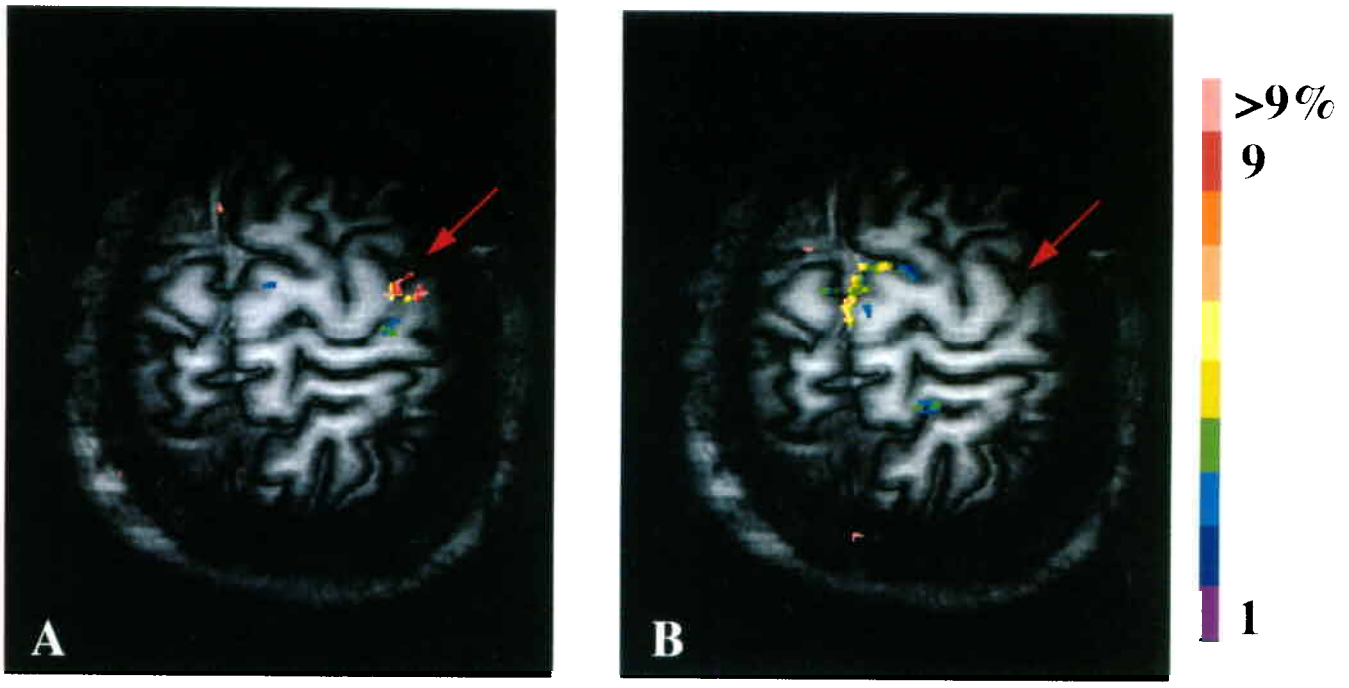

Plate 5. Functional activation amps ($p<0.001$) of finger (A) and toe movement (B) paradigms. Top is anterior and the red arrows indicate the central sulcus.

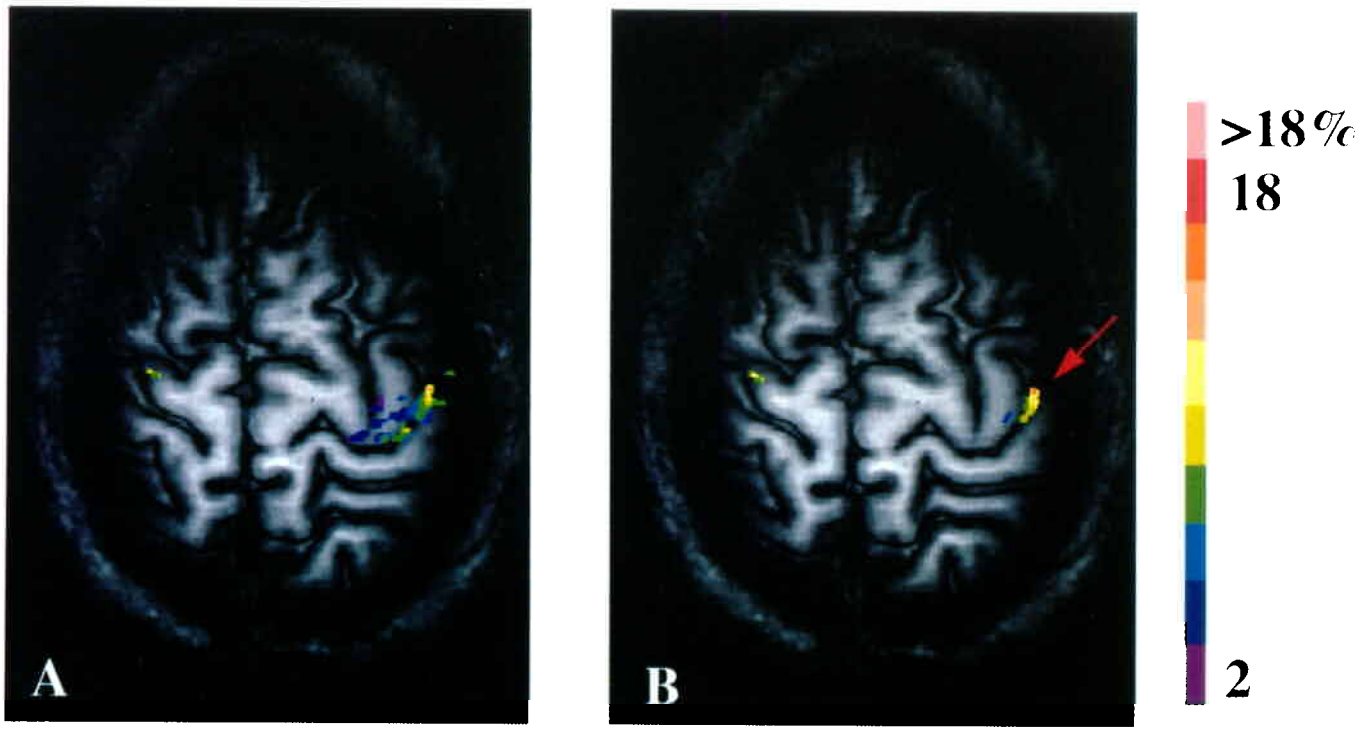

Plate 6. Functional activation maps ($p<0.001$) generated from navigator-echo T_2^*-weighted images with (A) and without (B) navigator-echo based motion correction, overlaid on a T_1-weighted image. The red arrow indicates the central sulcus and top anterior